Modelling and characterization of optical micro-machined ultrasound sensors with a silicon photonic ring resonator in a buckled acoustical membrane

W.J. Westerveld[1,2], S.M. Leinders[2], P.L.M.J. van Neer[2,3], B. Snyder[1,4], H.P. Urbach[2], N. de Jong[2], M.D. Verweij[2], X. Rottenberg[1], V. Rochus[1]

[1] Imec, Kapeldreef 75, 3001 Leuven, Belgium
[2] Delft University of Technology, Dept. ImPhys, Lorentzweg 1, 2628 CJ Delft, The Netherlands
[3] TNO, Oude Waalsdorperweg 63, 2597 AK Den Haag, The Netherlands
[4] Formerly at Tyndall National Institute, Photonics Building, Lee Maltings, Cork, Ireland

Future applications of ultrasonography in (bio-)medical imaging require ultrasound sensor matrices with small sensitive elements. Promising are opto-mechanical ultrasound sensors (OMUS) based on a silicon photonic ring resonator embedded in a silicon-dioxide acoustical membrane. This work presents new OMUS modelling: acousto-mechanical non-linear FEM and photonic circuit equations. We show that initial wafer stress needs to be considered in the design: the acoustical resonance frequency changes considerably and OMUS sensitivity differs for up- or downwards buckled membranes. Simulated acoustical resonance frequency agrees well with measurements, assuming realistic SOI wafer stress. Measured sensitivity showed large device-to-device variation and simulations agree within this order of magnitude. We conclude that careful modeling of stress is necessary for the design of robust and sensitive sensors.

Introduction

Ultrasonography is widely used in (bio-)medical imaging and photo-acoustic imaging is rapidly advancing [1, 2]. Future applications require a matrix of small and sensitive ultrasound sensors. Many require thin and flexible cabling, e.g. catheter-based imaging or studies of moving rodents. Especially photo-acoustic imaging requires low-noise sensors, because the ultrasound waves generated by laser pulses are much weaker than in pulse-echo ultrasonography [3]. Traditional transducer arrays use piezo-electric material. However, fabrication and wiring of many small piezo-electric elements is challenging [1], each element requires an individual coaxial wire, and sensitivity of small sensors is limited [3]. One solution to overcome wiring and fabrication is to place the ultrasound sensor array on an ASIC [4]. Micro-machined ultrasound sensors with capacitive (CMUT) and piezo-electric (PMUT) read-out overcome fabrication difficulties by using wafer-scale MEMS fabrication. However, typical read-out still requires a coaxial wire per element and sensitivity is similar to piezo-electric transducers. A variety of optical ultrasound sensors has been demonstrated, see e.g. [5]. We previously demonstrated, at 1 MHz, a new type of opto-mechanical ultrasound sensor consisting of an acoustically resonant membrane with integrated silicon photonic ring resonator (fig 1) [6]. The measured detection limit of 0.4 Pa is similar to the state-of-the-art of piezo-electric transducers while having a 65 times smaller footprint. This sensor was fabricated with wafer-scale CMOS and MEMS processes, suitable for matrix sensors. Read-out of many sensors via a single optical fiber is envisioned using silicon photonic wavelength-division multiplexing [7].

Device and fabrication

The sensor (Fig 1) consists of a silicon photonic resonator in an acoustically resonant silicon dioxide membrane. Devices are fabricated in a silicon-on-insulator (SOI) wafer

with a 0.22 μm thick silicon waveguide layer, a 2 μm thick buried oxide (BOX) layer, and a thick silicon substrate. The photonic circuitry was fabricated at Imec via ePIXfab Silicon Photonic MPW (now part of Europractice IC Service). This wafer was diced for further MEMS processing at TNO. A 0.5 μm thick silicon-dioxide protective cladding was deposited at using PECVD. Then the membrane was etched from the back-side of the wafer-die using a deep reactive ion etch (Bosch process) with the silicon-dioxide layer as chemically selective etch stop. The chips were glued on glass plates for mechanical stability, with a 4-mm hole below the membrane. The opto-mechanical chips were fiber-coupled at Tyndall National Institute with coated fiber array blocks for underwater application [8]. The BOX layer of SOI wafer has a high initial compressive stress, typically between -400 MPa and -200 MPa [9]. The initial stress of the PECVD deposited SiO2 layer is expected between -300 MPa and 0 MPa [10]. This causes mechanical buckling of the membrane. White-light interferometry (Bruker ContourGT-K) showed a deflection of approximately 4 μm.

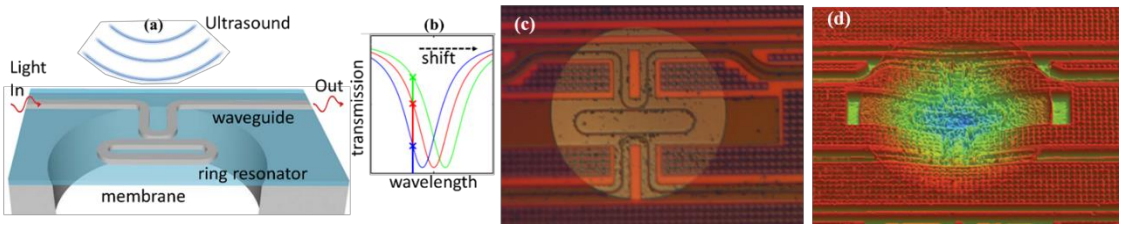

Fig 1. Opto-mechanical ultrasound sensor (OMUS). **(a)** Ultrasound waves impinge on the membrane thereby stretching the membrane with integrated silicon photonic ring resonator. This dynamically shifts the ring resonance wavelengths. **(b)** Read-out principle: the wavelength of a laser is tuned to the resonance flank. The sound-induced resonance shift translates to an intensity modulation of the transmitted light. Resonance around wavelength 1550 nm. **(c)** optical microscope picture of a similar sensor. **(d)** White-light interferometry showing bucking of ~4 μm. **(all)** Racetrack-shaped resonators with straight sections of 40 μm, bend radius 5 μm, and 2 directional couplers with ~5% coupling. Membrane diameters 60 – 130 μm.

Theory and modeling

To get insight in the bending of the membrane, two limiting cases are relevant. In thin plates with small deflections, one can neglect in-plane forces and stretching of the neutral plane (the mid-plane for a homogenous plate). The mechanics are dictated by the flexural rigidity of the plate, i.e. the resistance to bending due to compression or elongation away from the neutral plane (Fig 2a). In contrast, for infinitely thin plates, possibly with large deflections, mechanics is dictated by stretching of the neutral plane (like a balloon). Our sensor membranes have both flexural rigidity and in-plane stress due to initial compressive stress. See e.g. Fig 2b, the mid-plane has ~0.2% elongation while upper and lower planes have larger compression or elongation. For unbuckled membranes, flexural rigidity acts against bending while compressive in-plane stress acts to bend the membrane. For some initial stress, the opposing effects have similar strength and the membrane bends easily under tangential load (fig 2c,e).

Non-linear static deflection of a homogenous SiO_2 membrane was modeled in 2-D axisymmetric FEM using Comsol's Solid Mechanics module. To arrive at the correct solution, first a large tangential boundary load was applied with initial wafer stress away from buckling. This solution was updated for gradually changing load and stress towards the desired configuration (Fig 2b). Acousto-mechanical behavior was modeled as time-harmonic perturbation to the pre-stressed solution, where the upper hemisphere (water) was modeled using the Acoustics module (Fig 2c). Incident pressure of 1 Pa was modeled as membrane boundary load of 2 Pa. We found this to be a good approximation for a

1 Pa incident planewave with corresponding reflection. The center deflection $w(r=0)$, was computed for a sweep of frequency f, from which the resonance was extracted (Fig 2f). The optical power transmission $T(\theta, ..)$ from the input to the output of the waveguide that is coupled to the resonator depends, among others, on the optical phase delay of a ring round-trip $\theta = -2\pi\, n_e(\lambda)\, l / \lambda$, with λ the vacuum wavelength, n_e the effective index, n_g the effective group, and l the circumference of the ring [11]. The ring has resonances when $\theta_r = 2\pi m$ for integer m. We linearize $\theta(\lambda)$ in λ around resonance, i.e. $\Delta\theta \approx \partial\theta/\partial\lambda \cdot \Delta\lambda$, where $\partial\theta/\partial\lambda = 2\pi\, n_g\, l / \lambda^2$. Stretching the waveguide causes a change in effective index n_e and circumference l, hence a change in the phase delay θ at given wavelength λ and also a shift in resonance wavelength. In this work we neglect the change in effective index n_e, although this may contribute a factor 1/3rd or more to the resonance shift [12, 13]. With spectral slope $\partial T/\partial\lambda$ extracted from a measured spectrum, n_e and n_g computed, we find the change in optical transmission due to a deformation-induced change in circumference: $\partial T/\partial l = (\partial T/\partial\lambda)(\partial\lambda/\partial\theta)(\partial\theta/\partial l) = (\partial T/\partial\lambda)(n_e \cdot \lambda)/(n_g \cdot l)$. The sound-induced circumference change Δl was found from acousto-mechanical FEM simulations of membrane deformation, described by strain tensor $S(r)$ at depth 0.5 mm below the membrane surface.

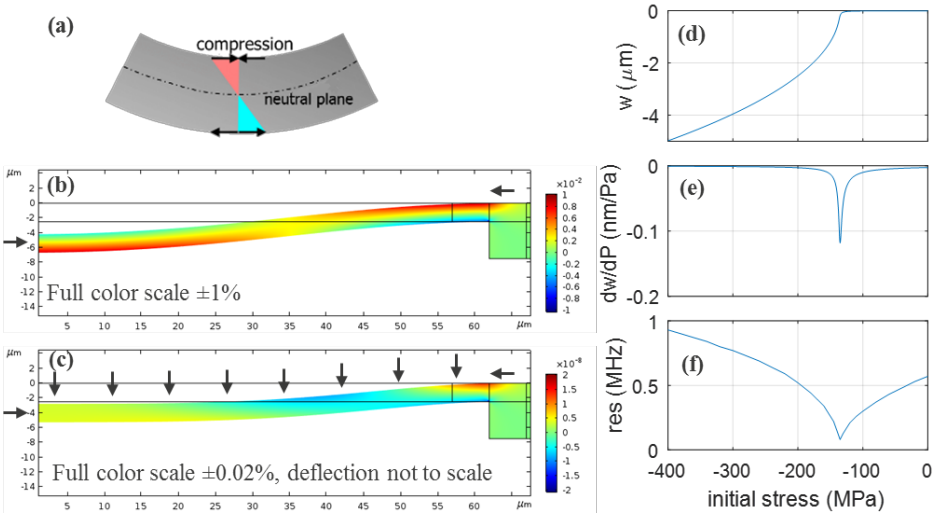

Fig. 2. Simulated membrane bending (diameter 124 μm, stress -320 MPa). **(a)** Sketch of pate bending. **(b,c)** strain tensor rr-component. **(b)** Buckled membrane due to initial stress. **(c)** Incremental strain due to transversal load, in this case an 800 kHz ultrasonic pressure wave of 1 Pa. **(d)** Deflection due to initial stress. **(e)** Deflection of the stressed membrane due to static transversal uniform load of 1 Pa. **(f)** Membrane resonance frequency in water.

Measurements and results

Fabricated sensors were submerged in water, either for OMUS measurements [6] or for simultaneous OMUS and membrane-displacement measurements using a laser vibrometer (see Ref. [14]). Simultaneous recording of OMUS signal and displacement show good correspondence (Fig. 3a). Measured acoustical resonance frequencies (Fig. 3c) agree with simulations for realistic compressive stress in the range -400 to -300 MPa. The resonances cannot be explained by thickness variation (2.25 to 3.0 μm). For membrane diameters 70 to 82 μm, the buckling point occurs between -400 and -300 MPa, resulting in a flexible membrane with low resonance frequency (e.g. Fig 3c). Two devices with identical designs (#1 and #11) show similar measured resonance frequencies, however OMUS sensitivity differs strongly (a factor ~5, see Fig 3, table). We cannot explain this large difference, which precludes a precise comparison of modeling and measurements. Also, the buckling state of measured membranes is unknown. In Fig 3,

table, the wafer stress in FEM was chosen to fit the measured resonance frequency. Modeled and measured membrane displacement and OMUS sensitivity, both at resonance, have the same the order of magnitude. Simulations reveal that the sensitivity of downwards buckled membranes are lower, explained from Fig 2c where the radial strain at the top surface is tensile at r=0 µm but compressive at r=25 µm.

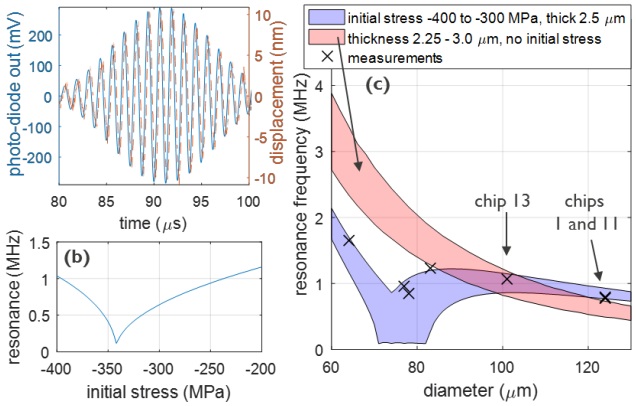

Diameter 124 µm Resonance 0.8 MHz	**Stress MPa**	**Displacement nm/kPa**	**Sensitivity dT/dP, kPa^{-1}**
Model, buckled up	-320	23	0.30
Model, buckled down	-320	25	0.16
Measured (chip I)	x	x	0.65 to 0.75
Measured (chip II)	x	10.8	0.16
Diameter 101 µm Resonance1.1 MHz	**Stress MPa**	**Displacement nm/kPa**	**Sensitivity dT/dP, kPa^{-1}**
Model, buckled up	-370	17.5	0.18
Model, buckled down	-370	17.6	0.005
Measured (chip 13)	x	8.2	0.08

Fig 3. (a) Time-trace of ultrasound pulse measurement, OMUS signal (blue, solid) and simultaneous interferometer displacement recording (red, dashed). **(b)** FEM simulation of a 77 µm membrane resonance frequency as function of initial stress in BOX. **(c)** Measured and modeled membrane resonances. Model without initial stress (pink, thickness range). Model with initial stress (purple, stress -400 to -300 MPa).

Discussion and conclusion

This work shows that initial stress needs to be considered in the design of opto-mechanical (ultrasound) sensors that use the buried oxide (BOX) layer of silicon-on-insulator (SOI) wafers. Modeled resonance frequencies for realistic initial BOX stress agree well with measurements. Measured OMUS sensitivity varies strongly from device to device, nonetheless we conclude that the modeling predicts the correct order of magnitude. For better understanding, it is necessary to improve fabrication and metrology (possibly etched BOX layer, PECVD SiO_2 thickness and conformity, back-side etch alignment, material properties, bucking, ...) and elaborate modeling (including e.g. strain-induced waveguide effective index change, non-uniform silicon waveguide layer in mechanical modeling). We believe the described modeling is an important step towards OMUS design optimization. Moreover, careful design and fabrication opens opportunities for flexible mechanical structures with a much smaller footprint.

References

[1] T.L. Szabo, *Diagnostic ultrasound imaging: inside out*, 2nd, Academic Press, 2014.
[2] L. V. Wang and J. Yao, *Nat. Methods* 13, 627–638 (2016).
[3] A. M. Winkler, K. Maslov, and L. V Wang, *J. Biomed. Opt.* 18, 097003 (2013).
[4] J. Janjic et al, *IEEE Trans. Ultrasonics, Ferroelectrics, and Frequency Control* 65, 1832 (2018).
[5] G. Wissmeyer et al, *Light Sci. Appl.* 7, 53 (2018).
[6] S. M. Leinders et al., *Scientific Reports* 5, 14328 (2015). (doi: 10.1038/srep14328)
[7] S. Pathak, *Silicon Nano-Photonics Based Arrayed Waveguide Gratings*, Ph.D. Thesis (2014).
[8] B. Snyder and P. O'Brien, *IEEE Trans. Compon. Packag. Technol.* 3, 954 (2013).
[9] Lindroos et al., *Handbook of Silicon Based MEMS Materials and Technologies*, Elsevier, 2010.
[10] PECVD Overview from Oxford Instruments, in *Process Manual* of Marvell Nanofabrication Lab. of UC Berkeley (2013). Online: http://nanolab.berkeley.edu/public/manuals/process_manual.shtml
[11] W.J. Westerveld and H. P. Urbach, *Silicon Photonics: Electromagnetic theory*, IOP Publishing, 2017.
[12] W.J. Westerveld et al, *IEEE J. Sel. Top. in Quantum Electronics* 20, 5900110 (2014).
[13] C. Castellan et al, *Optics Express* 26, 4204 (2017).
[14] Leinders, *Characterization of a novel Optical Micro-machined Ultrasound Transducer*, PhD (2017).